1-1-2013

Driving magnetostructural transitions in layered intermetallic compounds

Jianli Wang
University of Wollongong, jianli@uow.edu.au

L Caron
Technische Universiteit Delft

S J. Campbell
University Of New South Wales, stewart.campbell@adfa.edu.au

S J. Kennedy
ANSTO

M Hofmann
Technical University Of Munich

See next page for additional authors

Driving magnetostructural transitions in layered intermetallic compounds

Abstract

We report the dramatic effect of applied pressure and magnetic field on the layered intermetallic compound Pr0.5Y0.5Mn 2Ge2. In the absence of pressure or magnetic field this compound displays interplanar ferromagnetism at room temperature and undergoes an isostructural first order magnetic transition (FOMT) to an antiferromagnetic state below 158 K, followed by another FOMT at 50 K due to the reemergence of ferromagnetism as praseodymium orders (TCPr). The application of a magnetic field drives these two transitions towards each other, whereas the application of pressure drives them apart. Pressure also produces a giant magnetocaloric effect such that a threefold increase of the entropy change associated with the lower FOMT (at TCPr) is seen under a pressure of 7.5 kbar. First principles calculations, using density functional theory, show that this remarkable magnetic behavior derives from the strong magnetoelastic coupling of the manganese layers in this compound. 2013 American Physical Society.

Keywords

intermetallic, layered, compounds, transitions, driving, magnetostructural

Disciplines

Engineering | Physical Sciences and Mathematics

Publication Details

Wang, J., Caron, L., Campbell, S. J., Kennedy, S. J., Hofmann, M., Cheng, Z., Md Din, M., Studer, A. J., Bruck, E. & Dou, S. X. (2013). Driving magnetostructural transitions in layered intermetallic compounds. Physical Review Letters, 110 (21), 217211-1-217211-5.

Authors

Jianli Wang, L Caron, S J. Campbell, S J. Kennedy, M Hofmann, Z X Cheng, M Md Din, A J. Studer, E Bruck, and S X. Dou

Driving Magnetostructural Transitions in Layered Intermetallic Compounds

J. L. Wang,[1,2,*] L. Caron,[3] S. J. Campbell,[4] S. J. Kennedy,[2,†] M. Hofmann,[5] Z. X. Cheng,[1] M. F. Md Din,[1] A. J. Studer,[2] E. Brück,[3] and S. X. Dou[1]

[1]*Institute for Superconductivity and Electronic Materials, University of Wollongong, Wollongong, New South Wales 2522, Australia*
[2]*Bragg Institute, ANSTO, Lucas Heights, New South Wales 2234, Australia*
[3]*Fundamental Aspects of Energy and Materials, Faculty of Applied Sciences, Technische Universiteit Delft, Mekelweg 15, 2629 JB Delft, Netherlands*
[4]*School of Physical, Environmental, and Mathematical Sciences, The University of New South Wales, Canberra, Australian Capital Territory 2600, Australia*
[5]*FRM-II, Technische Universität München, Lichtenbergstrasse 1, Garching, Germany 85747*

(Received 12 November 2012; published 23 May 2013; publisher error corrected 29 May 2013)

We report the dramatic effect of applied pressure and magnetic field on the layered intermetallic compound $Pr_{0.5}Y_{0.5}Mn_2Ge_2$. In the absence of pressure or magnetic field this compound displays interplanar ferromagnetism at room temperature and undergoes an isostructural first order magnetic transition (FOMT) to an antiferromagnetic state below 158 K, followed by another FOMT at 50 K due to the reemergence of ferromagnetism as praseodymium orders (T_C^{Pr}). The application of a magnetic field drives these two transitions towards each other, whereas the application of pressure drives them apart. Pressure also produces a giant magnetocaloric effect such that a threefold increase of the entropy change associated with the lower FOMT (at T_C^{Pr}) is seen under a pressure of 7.5 kbar. First principles calculations, using density functional theory, show that this remarkable magnetic behavior derives from the strong magnetoelastic coupling of the manganese layers in this compound.

DOI: 10.1103/PhysRevLett.110.217211 PACS numbers: 75.30.Sg, 61.05.fm, 71.20.Eh

The giant magnetocaloric effect (GMCE) as exhibited by rare-earth–transition-metal intermetallic compounds is characterized by a combination of a large magnetocaloric effect at a magnetic phase transition and field-induced first-order magnetic transitions and/or structural transitions at or near the magnetic ordering temperature [1,2]. The magnetic properties of ternary rare-earth RMn_2X_2 (with X = Ge or Si) compounds with the tetragonal $ThCr_2Si_2$-type structure ($I4/mmm$) have attracted interest in recent years due to their natural layered structure and the fact that they exhibit either coupled magnetic and crystallographic transitions or valence-related transitions [3–6]. Application of hydrostatic pressure has proved to be effective in the enhancement of magnetocaloric properties by increasing the magnitude and/or tuning the MCE to the desired temperature range in materials such as $R_5(Si_xGe_{1-x})_4$ [7], MnAs [8], $La(Fe_xSi_{1-x})_{13}$ [9], and RMn_2Ge_2 [10].

While fundamental magnetic properties such as saturation magnetization and magnetic structures have been widely reported for the RMn_2Ge_2 systems [e.g., Ref. [11]], less insight has been gained on the relationship between magnetovolume effects and the magnetic entropy at magnetic transitions. $Pr_{0.5}Y_{0.5}Mn_2Ge_2$ was selected for this study following our investigation of the $Pr_{1-x}Y_xMn_2Ge_2$ system [12] in which both the loss of moment in the Pr sublattice and the significant modifications of the magnetic states of the Mn lattice were investigated [13] because it exhibits reentrant ferromagnetism. Our investigation of the structural changes occurring in the reentrant ferromagnet $Pr_{0.5}Y_{0.5}Mn_2Ge_2$ using neutron diffraction in applied magnetic fields, combined with magnetic measurements under hydrostatic pressure has enabled us to develop a new insight into the magnetic behavior of this system and the role of magnetostructural coupling in the magnetocaloric effect.

Details of the preparation and characterization of the initial set of $Pr_{1-x}Y_xMn_2Ge_2$ compounds (x = 0.0–1.0) can be found in Refs. [6,12]. The temperature dependence of the dc magnetization, $M(T)$, was measured over the range 5–370 K using a superconducting quantum interference device (SQUID) and at hydrostatic pressures up to p = 7.5 kbar [14]. Neutron diffraction patterns were collected over the range ~10–355 K using the GEM diffractometer at ISIS (Rutherford Appleton Laboratory, UK) [12] and the Wombat diffractometer (λ = 2.4072 Å) at the OPAL reactor (ANSTO, Australia). Reentrant ferromagnetism appears in $Pr_{0.5}Y_{0.5}Mn_2Ge_2$ producing first-order magnetostructural phase transitions.

From our combined magnetization and neutron diffraction studies, four magnetic phase transitions have been detected in $Pr_{0.5}Y_{0.5}Mn_2Ge_2$. On cooling from the paramagnetic region, the first transition from the paramagnetic state (PM) to the intralayer antiferromagnetic (AFl) state occurs at $T_N^{intra} \sim 375$ K with the second transition from the AFl magnetic structure to a canted ferromagnetic spin structure (Fmc) occurring at $T_C^{inter} \sim 343$ K. On cooling below $T_N^{inter} \sim 158$ K the Fmc magnetic structure gives way to the antiferromagnetic mixed commensurate magnetic structure (AFmc) before the onset of ordering of the

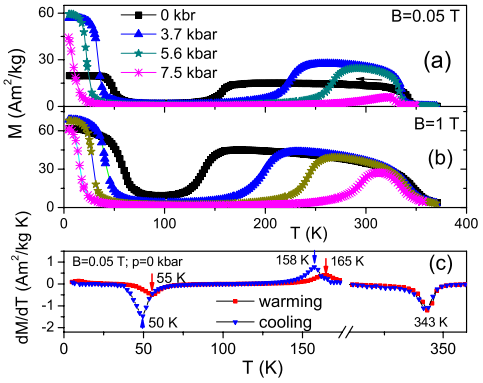

FIG. 1 (color online). (a) Temperature dependence of the magnetization of $Pr_{0.5}Y_{0.5}Mn_2Ge_2$ as measured on cooling in magnetic field of $B = 0.05$ T (a) and $B = 1$ T (b) under applied pressures in the range $p = 0 - 7.4$ kbar as well as (c) dM/dT obtained upon cooling and warming at ambient pressure, showing hysteresis at T_N^{inter} and T_C^{Pr}.

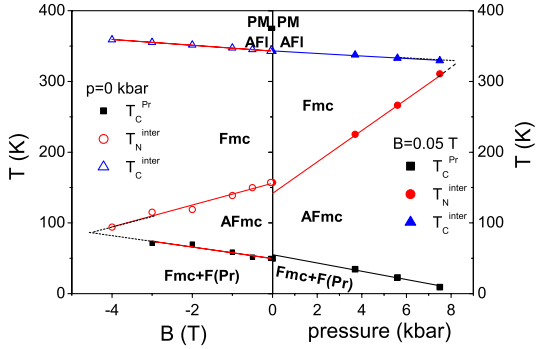

FIG. 2 (color online). Magnetic phase diagram of $Pr_{0.5}Y_{0.5}Mn_2Ge_2$ as a function of applied magnetic field at ambient pressure (left part) and applied pressure (right part) (the magnetic transition temperatures T_C^{inter}, T_N^{inter} and T_C^{Pr} were determined from cooling runs in a field of $B = 0.05$ T). The lines through the data act as guides to the eye.

Pr magnetic sublattice [F(Pr)] below $T_C^{\text{Pr}} \sim 50$ K and formation of the combined region [Fmc + F(Pr)] (see details in the Supplemental Material [15]).

Figures 1(a) and 1(b) show the temperature dependence of magnetization for $Pr_{0.5}Y_{0.5}Mn_2Ge_2$ on cooling in a magnetic field B = 0.05 T and 1 T and under applied pressures in the range $p = 0$–7.5 kbar, respectively. Comparison of the cooling and warming measurements at ambient pressure as shown by the derivative of magnetization with respect to temperature [in Fig. 1(c)] clearly shows hysteresis in the phase transitions at T_N^{inter} and T_C^{Pr}—indicative of first-order magnetic transitions (FOMT). Analyses by Arrott plots of the isothermal magnetization data measured around T_N^{inter} and T_C^{Pr} confirm the first order nature of these two transitions (see the Supplemental Material [15]).

Given that the magnetic structure in RMn_2Ge_2 and related systems depends sensitively on composition and the intraplanar Mn-Mn spacing [3–6,16], the difference in the transition temperatures between those reported earlier [13] and the present study can be understood in terms of the possible compositional variations. Similarly, the magnetization closely approaches zero in the antiferromagnetic region between T_N^{inter} and T_C^{Pr} for the present sample [Fig. 1(a)] when compared with previous results [13].

Figure 2 shows the phase diagram of $Pr_{0.5}Y_{0.5}Mn_2Ge_2$ as a function of magnetic field (left side) and applied pressure (right side). The transition temperatures (T_C^{inter}, T_N^{inter}, and T_C^{Pr}) were determined from the magnetization on cooling. Figure 2 reveals that while T_N^{inter} increases sharply with applied pressure, both T_C^{inter} and T_C^{Pr} decrease with pressure. These changes, indicate that applied pressure stabilizes the antiferromagnetic state but weakens the ferromagnetic state, illustrating the fact that a shorter Mn-Mn intraplanar distance favors the antiferromagnetic c-axis coupling [17]. Noting that lower chemical pressure [18] also decreases the Mn-Mn intraplanar distance and stabilizes antiferromagnetic coupling between the Mn moments, we can consider the influence of applied pressure to be analogous to chemical pressure. To quantify the relative impact of chemical pressure and applied pressure on the magnetic order we express the response to substitution of 50% of Pr with Y in $Pr_{1-x}Y_xMn_2Ge_2$ in terms of applied pressure; noting that the cell volume of $Pr_{0.5}Y_{0.5}Mn_2Ge_2$ is 2.2% less than that of $PrMn_2Ge_2$ [13]. We then calculate the pressure dependence of cell volume of $PrMn_2Ge_2$ using the bulk modulus and its pressure derivative from isostructural RT_2X_2 compounds [19] to obtain a value of p = 19.5 kbar for the equivalent pressure difference between $PrMn_2Ge_2$ and $Pr_{0.5}Y_{0.5}Mn_2Ge_2$. Thus, noting that $T_C^{\text{Pr}} = 100$ K in $PrMn_2Ge_2$ [12,13], we calculate that the rate of change of T_C^{Pr} due to chemical pressure in $Pr_{0.5}Y_{0.5}Mn_2Ge_2$ (dT_C^{Pr}/dp) is—2.6 K/kbar, which is around 1/2 the measured response to applied pressure. This comparison highlights the fact that electronic interactions also contribute to the response to chemical substitution. In this case, the magnetic states are also modified due to introduction of the nonmagnetic element Y and to differences in the electron configurations of Pr^{3+} ($4f^2$) and Y^{3+} ($4d^0$) ions.

In direct contrast to the effect of pressure, applied magnetic field enhances the ferromagnetic coupling between layers, leading to increases in the Curie temperatures (T_C^{inter} and T_C^{Pr}) and a corresponding decrease in the antiferromagnetic transition temperature with magnetic field. The rates of change for the three transitions are: $dT_N^{\text{inter}}/dB = -15.4$ K/T, $dT_C^{\text{Pr}}/dB = +8.1$ K/T and $dT_C^{\text{inter}}/dB = +4.1$ K/T. The opposite effect of applied pressure and magnetic field on these magnetic phase transitions can be understood in the terms of magnetoelastic coupling. This manifests as spontaneous magnetostriction in the absence of either pressure or magnetic field, as forced magnetostriction under applied pressures and as induced magnetostriction under applied magnetic field.

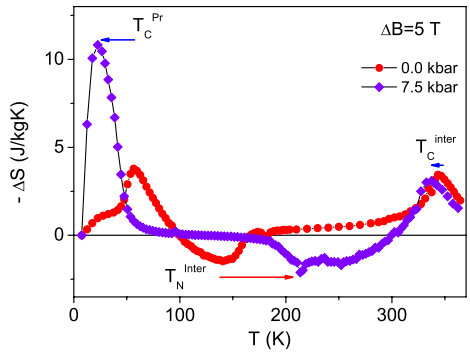

FIG. 3 (color online). Temperature dependence of isothermal magnetic entropy change $(-\Delta S)$ of $Pr_{0.5}Y_{0.5}Mn_2Ge_2$ as determined with a field change of $\Delta B = 5$ T in different pressures. Arrows indicate shift of critical temperature with pressure.

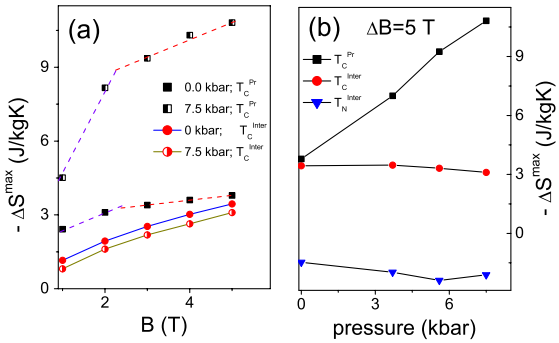

FIG. 4 (color online). The maximum entropy change of $Pr_{0.5}Y_{0.5}Mn_2Ge_2$ (a) as a function of magnetic field at $p =$ 0 kbar and 7.5 kbar and (b) as a function of pressure with a field change of $\Delta B = 5$ T.

In Fig. 2 we have extrapolated the T_C^{Pr} and T_N^{inter} lines to the point of intersection at an applied magnetic field of ~4.5 T. This is the critical field at which antiferromagnetic interplanar coupling disappears completely. We have also extrapolated the T_N^{inter} and T_C^{inter} lines to the point of intersection at an applied pressure of ~8.5 kbar. This is the critical pressure at which ferromagnetic interplanar coupling disappears completely. We note also that this is quite close to the pressure at which ferromagnetic ordering of Pr is completely suppressed.

The magnetic entropy changes $-\Delta S$ around T_C^{Pr}, T_N^{inter}, and T_C^{inter} have been derived from magnetization data for a magnetic field change (ΔB) of 5 T under various applied pressures. Selected curves of $-\Delta S$ are shown in Fig. 3, where we see that $-\Delta S$ is positive around T_C^{Pr} and T_C^{inter} but negative (inverse magnetocaloric effect) around T_N^{inter}. The $-\Delta S_{\mathrm{max}}$ around T_C^{Pr} has been strongly enhanced by the application of pressure [see also Fig. 4(b)] while the $-\Delta S_{\mathrm{max}}$ values around T_N^{inter} and T_C^{inter} remain essentially unchanged for the same pressure change. The maximum values of the magnetic entropy change $-\Delta S_{\mathrm{max}}$ around T_C^{Pr}, T_N^{inter}, and T_C^{inter} are shown as functions of the magnetic field in Fig. 4(a) and of pressure in Fig. 4(b). The magnetic entropy change is proportional to the integral of dM/dT with respect to the applied field. Therefore a pressure change that sharpens the magnetization curve will also increase the entropy change. Thus the strong dependence of entropy on pressure around T_C^{Pr} is consistent with the sharpening of the magnetization curve under pressure as seen in Fig. 1. In contrast, we note that pressure has little effect on the magnitudes of either dM/dT or $-\Delta S$ around T_N^{inter} and T_C^{inter}. The large shift of the peak in $-\Delta S$ around T_C^{Pr} to lower temperature and even larger shift of T_N^{inter} to higher temperature with increasing pressure, agrees well with the behaviors of T_C^{Pr} and T_N^{inter} in Fig. 2. The peak in $-\Delta S$ associated with the lower FOMT is ~8 K above T_C^{Pr} regardless of pressure, indicating localized reorientation of some Mn moments above the phase transition. This is not surprising in a pseudoternary compound such as this, where there is a solid solution of Pr and Y on the rare earth site. The nature of the solid solution is such that there are random variations in Pr-Y concentration, producing local strain fields and hence short ranged variations in the Mn-Mn magnetic exchange interaction. We have recently reported evidence of local strain fields and the predominance of mixing of AF*mc* and F*mc* states in pseudoternaries of RMn_2X_2 compounds [18].

Comparison of the lattice parameters of $Pr_{0.5}Y_{0.5}Mn_2Ge_2$ at 300 K ($a = 4.067$ Å) with other systems displaying reentrant ferromagnetism such as $SmMn_2Ge_2$ ($a =$ 4.045 Å) [20], $NdMn_{1.575}Fe_{0.425}Ge_2$ ($a = 4.081$ Å) [17] and $PrMn_{1.4}Fe_{0.6}Ge_2$ ($a = 4.088$ Å) [19], we note a range of a lattice parameter from 4.045 to 4.088 Å, corresponding to a variation of Mn-Mn nearest neighbor distance $d_{\mathrm{Mn\text{-}Mn}}$ of over 1%. This demonstrates that while geometric criteria are significant in determining the magnetic structures of RMn_2Ge_2 and related systems, electronic interactions from the different elements present also play a vital role [19]. Figure 5 shows the variation of the lattice parameters of $Pr_{0.5}Y_{0.5}Mn_2Ge_2$ with temperature in zero field and in an applied magnetic field of 4 T. The zero field data [Figs. 5(a) and 5(b)] reveal that anisotropic lattice changes occur around T_C^{Pr} and T_N^{inter} revealing the presence of a strong magneto-volume effect (spontaneous magnetostriction) associated with the transitions between F*mc* and AF*mc* states, as also observed in related systems [6,18,20,21]. Due to reorientation of crystallites under magnetic field, only the a lattice parameter could be derived accurately from the neutron diffraction patterns collected in an applied magnetic field (B) of 4 T. Figure 5(a) shows that, compared with the data for $B = 0$ T, the lattice parameter a for $B =$ 4 T does not exhibit obvious dependence on the magnetic state. As shown in Fig. 5(c), the response of the a lattice parameter to applied magnetic field was clarified further by collecting neutron patterns at the different temperatures under various magnetic fields. It is clear that the lattice parameter a remains essentially invariant in the ferromagnetic (F*mc*) state (at $T = 40$ K and between 225 and 320 K)

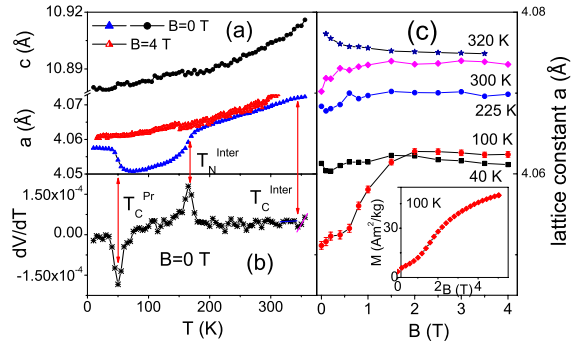

FIG. 5 (color online). Temperature dependence of lattice parameters as measured by neutron diffraction for $B = 0$ T and $B = 4$ T. (a) lattice parameters a, c ($B = 0$ T) and a parameter ($B = 4$ T); (b) dV/dT ($B = 0$ T) and (c) a lattice parameter as a function of magnetic field at selected temperatures. The inset to Fig. 5(c) shows the magnetization curve of $Pr_{0.5}Y_{0.5}Mn_2Ge_2$ at 100 K.

while in the antiferromagnetic (AFmc) state (at $T =$ 100 K), a increases with applied field approaching saturation at ~2 T. This field induced magnetostriction shows similar trends to the magnetization curve measured at the same temperature [see inset to Fig. 5(c)], providing direct evidence that the unit cell is larger in a ferromagnetic state than in an antiferromagnetic state [18–21] Application of a magnetic field in the AFmc state region therefore induces both a magnetic phase transition from AFmc to Fmc and simultaneously increases the lattice parameter a [Fig. 5(c)].

The observed magnetic properties and the relationship between the critical temperature, magnetic field, and pressure can be explained using standard thermodynamic relations. For the second-order phase transition (T_C^{inter}) the Ehrenfest relation applies [17],

$$dT_C/dP = TV^*(\Delta\alpha_V/\Delta C_p), \tag{1}$$

where V is the volume, $\Delta\alpha_V$ is the difference between the thermal expansion coefficients above and below the transition, and ΔC_p is the magnitude of the specific heat anomaly at the phase transition (see Fig. 3S in the Supplemental Material [15]). The plot of $\delta V/\delta T$ [Fig. 5(b)] dips at T_C^{inter} indicating that $\Delta\alpha_V < 0$, and hence that dT_C^{inter}/dP is also below zero, consistent with observations (Fig. 2).

For the first-order magnetic phase transitions at T_N^{inter} (Fmc to AFmc) and at T_C^{Pr} (AFmc to [F(Pr) + Fmc)], the Clausius-Clapeyron thermodynamic relation applies [14],

$$dT_{\text{crit}}/dP = -\Delta V/\Delta M^*(dT_{\text{crit}}/dB). \tag{2}$$

Using the experimental values for the Fmc to AFmc phase transition of $dT_N^{\text{inter}}/dP = 22.2$ K/kbar, $dT_N^{\text{inter}}/dB = -15.4$ K/T and $\Delta M = -27.3$ A m^2/kg derived from the magnetic measurements, we estimate the change in the unit cell volume at T_N^{inter} to be $\Delta V = 3.93 \times 10^{-7}$ m^3/kg. This leads to a calculated value at T_N^{inter} of $\Delta V/V = -0.27\%$, in good agreement with $\Delta V/V = -0.25\%$ derived from the neutron diffraction study [Fig. 5(b)]. Similarly, for the transition at T_C^{Pr}, the values of $dT_C^{\text{Pr}}/dP = -5.8$ K/kbar, $dT_C^{\text{Pr}}/dB = 8.1$ K/T and $\Delta M = 30.9$ A m^2/kg lead to $\Delta V = 4.32 \times 10^{-7}$ m^3/kg. This in turn leads to $\Delta V/V = 0.30\%$, again in good agreement with the measured value of $\Delta V/V = 0.29\%$ from the neutron diffraction study.

For first order magnetic phase transitions, the total field-induced magnetic entropy change ΔS_{tot} can be expressed as the sum of the conventional second-order magnetic entropy change (ΔS_M) and the entropy difference between the two crystallographic states (ΔS_{st}), i.e., $\Delta S_{\text{tot}} = \Delta S_M + \Delta S_{\text{st}}$ [22]. In the case of $Pr_{0.5}Y_{0.5}Mn_2Ge_2$, the unit cell volume of the magnetic states before and after the first-order magnetic transition are significantly different indicating a structural entropy change at T_C^{Pr}. As discussed by Gschneider *et al.* [22], on completion of a magnetic field induced structural transition, i.e., when 100% of the volume of the sample is converted from one state to another, the structural entropy difference of the two magnetic states (ΔS_{st}) must remain field independent. Figure 5(c) shows that an applied field of ~2 T is sufficient to complete the structural transition associated with the change from the antiferromagnetic state to a ferromagnetic state at $T = 100$ K. This observation correlates with the observed change in slope in the magnetic field dependence of the maximum entropy change at $B \sim 2$ T [Fig. 4(a)], indicating that the structural contribution to the magnetic entropy change is complete by 2 T. Applying the relationship between structural entropy change and relative volume change from Ref. [22] [i.e., $\delta(\Delta V/V)/\delta(\Delta S_{\text{st}}) = 8 \times 10^{-4}(\text{J/kg K})^{-1}$], our experimentally observed volume changes of $\Delta V/V = 0.29\%$ and 0.25% at T_C^{Pr} and T_N^{inter} would correspond to structural entropy contributions of $\Delta S_{\text{st}} = 3.6$ J/kg K and 3.1 J/kg K, respectively, which indicates the structural entropy contributes significantly to the total entropy at both transitions.

First principles calculations of the electronic structure of the two magnetic states (AFmc and Fmc) have been carried out using a spin polarized localized density approximation (LSDA) in the framework of density functional theory (DFT) [23]. For these calculations the magnetic structures of AFmc and Fmc states and temperature dependence of lattice parameters from neutron diffraction and the pressure dependence of lattice parameters from synchrotron x-ray diffraction (see Fig. 9S in the Supplemental Material [15]) were used as input. The calculations show that changes to the magnetic energy of the two states are caused directly by modification of the lattice with temperature and pressure. Because of the anisotropic nature of the response of the lattice to changes in temperature and pressure, corresponding changes in the magnetic exchange energy of the two states have different dependencies. Calculated thermal and pressure dependence of the relative energies of the two states shows remarkable agreement with our experimental results. Specifically the DFT calculations

indicate that the F*mc* state is favored (with lower relative energy) at ambient pressure below ~50 K and above ~150 K, whereas the AF*mc* state is favored between those temperatures. At 300 K the local density of states shows that the *d* bands of the Mn atoms in the AF*mc* state narrow more under high pressure than they do in the F*mc* state. Thus, whereas F*mc* is favored at ambient pressure, AF*mc* is favored above ~4 kbar.

In conclusion, we have investigated the dramatic effect of applied pressure and magnetic field on the layered intermetallic compound $Pr_{0.5}Y_{0.5}Mn_2Ge_2$, constructing magnetic phase diagrams, and probing the nature of the different responses at the magnetic transitions T_C^{inter}, T_N^{inter}, and T_C^{Pr} to hydrostatic pressure and magnetic field. Our findings, which are consistent with spin-polarized DFT theory, show that application of magnetic field and pressure stabilize the ferromagnetic and antiferromagnetic interlayer order, respectively. The magnetic entropy change around the FOMT at $T_C^{\text{Pr}} \sim 50$ K, where magnetostructural coupling plays a significant role, is enhanced by a factor of ~2.8 at a pressure of 7.5 kbar.

J. L. W., S. J. C., and M. H. acknowledge the assistance of Professor P. Radaelli during experiments at GEM, ISIS. This work is supported in part by Discovery Grants DP0879070; DP110102386 from the Australian Research Council, the Industrial Partnership Program I18 of the Dutch Foundation for Fundamental Research on Matter (FOM), and by a joint agreement between the ANSTO and the University of Wollongong. The work is also supported in part by a grant from the AINSE and the Access to Major Research Facilities Program.

*jianli@uow.edu.au
†sjk@ansto.gov.au

[1] K. A. Gschneidner, Jr., V. K. Pecharsky, and A. O. Tsokol, Rep. Prog. Phys. **68**, 1479 (2005).
[2] E. Brück, J. Phys. D **38**, R381 (2005); O. Tegus, E. Brück, K. H. J. Buschow, and F. R. de Boer, Nature (London) **415**, 150 (2002).
[3] B. Malaman, G. Venturini, A. Blaise, J. P. Sanchez, and G. Amoretti, Phys. Rev. B **47**, 8681 (1993).
[4] M. Hofmann, S. J. Campbell, and A. V. Edge, Phys. Rev. B **69**, 174432 (2004).
[5] T. Fujiwara, H. Fujii, and T. Shigeoka, Phys. Rev. B **63**, 174440 (2001).
[6] J. L. Wang, S. J. Campbell, J. M. Cadogan, A. Studer, R. Zeng, and S. X. Dou, Appl. Phys. Lett. **98**, 232509 (2011).
[7] L. Morellon, Z. Arnold, P. A. Algarabel, C. Magen, M. R. Ibarra, and Y. Skorokhod, J. Phys. Condens. Matter **16**, 1623 (2004).
[8] S. Gama, A. A. Coelho, A. de Campos, A. M. G. Carvalho, F. C. G. Gandra, P. J. von Ranke, and N. A. de Oliveira, Phys. Rev. Lett. **93**, 237202 (2004).
[9] Y. Sun, Z. Arnold, J. Kamarad, G. J. Wang, B. G. Shen, and Z. H. Cheng, Appl. Phys. Lett. **89**, 172513 (2006); B. G. Shen, J. R. Sun, F. X. Hu, H. W. Zhang, and Z. H. Cheng, Adv. Mater. **21**, 4545 (2009).
[10] P. Kumar, K. G. Suresh, A. K. Nigam, A. Magnus, A. A. Coelho, and S. Gama, Phys. Rev. B **77**, 224427 (2008).
[11] A. Szytula and J. Leciejewicz, in *Handbook on the Physics and Chemistry of Rare Earths*, edited by K. A. Gschneider, Jr. and L. Erwin (Elsevier, Amsterdam, 1989), Vol. 12, p. 133; A. Szytula, J. Leciejewicz, *Handbook of Crystal Structures and Magnetic Properties of Rare Earth Intermetallics* (CRC, Boca Raton, 1994).
[12] J. L. Wang, S. J. Campbell, M. Hofmann, S. J. Kennedy, M. Avdeev, M. F. Md Din, R. Zeng, Z. X. Cheng, and S. X. Dou, J. Appl. Phys. **113**, 17E147 (2013).
[13] Y. G. Wang, F. M. Yang, C. P. Chen, N. Tang, and Q. D. Wang, J. Phys. Condens. Matter **9**, 8539 (1997).
[14] L. Caron, N. T. Trung, and E. Brück, Phys. Rev. B **84**, 020414(R) (2011).
[15] See the Supplemental Material at http://link.aps.org/supplemental/10.1103/PhysRevLett.110.217211 for a complete presentation of the raw data and details of analysis.
[16] G. Venturini, B. Malaman, and E. Ressouche, J. Alloys Compd. **237**, 61 (1996)
[17] E. G. Gerasimov, N. V. Mushnikov, and T. Goto, Phys. Rev. B **72**, 064446 (2005).
[18] J. L. Wang, S. J. Kennedy, S. J. Campbell, M. Hofmann, and S. X. Dou, Phys. Rev. B **87**, 104401 (2013).
[19] J. L. Wang, S. J. Campbell, A. J. Studer, M. Avdeev, M. Hofmann, M. Hoelzel, and S. X. Dou, J. Appl. Phys. **104**, 103911 (2008).
[20] G. J. Tomka, C. Ritter, P. C. Riedi, Cz. Kaputska, and W. Kocemba, Phys. Rev. B **58**, 6330 (1998).
[21] J. L. Wang, S. J. Campbell, A. J. Studer, M. Avdeev, R. Zeng, and S. X. Dou, J. Phys. Condens. Matter **21**, 124217 (2009).
[22] K. A. Gschneidner, Jr., Y. Mudryk, and V. K. Pecharsky, Scr. Mater. **67**, 572 (2012).
[23] G. Kresse and J. Furthmuller, Phys. Rev. B **54**, 11169 (1996).